

PALAEOTECTONIC ENVIRONMENT AND LANDSLIDE PHENOMENA IN THE AREA OF MALAKASA, GREECE

Mourtzas N.D.¹ and Sotiropoulos E.²

¹GALIAERGON Ltd, Kefallinias Str. 16-18, 152 31 Chalandri, Athens, gaiaergon@gmail.com, nikosmourtzas@gmail.com

² GEOMECHANIKI S.A., Ethnikis Antistaseos Str. 91, 153 44 Pallini, Athens, geomsot@gmail.com

Abstract

The extended landslide of Malakasa area, located 35km to the North of Athens, occurred in a neopalaeozoic schist-sandstone klippe, a complex Palaeotectonic environment in the northern roots of Parnitha Mt. Due to this failure, railway line and highway connection between Athens and central and North Greece were cut off. In this paper, it is attempted to approach the landslide mechanism based on: (i) the kinematic data on the failure surface, (ii) the morphological features of the surface, (iii) the movement vectors, and (iv) the lithostratigraphy and hydro-geological features of the sliding mass. According to the above criteria, three soil blocks can be identified in the landslide mass, which are differentiated by their lithological structure, kinematic features, type of deformation and hydro-geological behavior. The causal factor of the extended landslide was the gradual loss of support of these three blocks and their slide on a pre-sheared surface of low strength that has been caused by the extended excavation in the slope toe. The palaeotectonic structure and the development and geometry of the geological formations in the landslide area were not taken into account during the construction of the drainage works, for slope stabilization and the increasing of safety factor, something which led to the over-designing of the remedial measures.

Key words: lithostratigraphy, upthrust, kinematic, groundwater, slope stabilization.

Περίληψη

Η εκτεταμένη κατολίσθηση στην περιοχή της Μαλακάσας, 35km βόρεια της Αθήνας, εκδηλώθηκε σε σχιστομαμιτικό ράκος των νεοπαλαιζωικών σχηματισμών, σε ένα πολύπλοκο παλαιοτεκτονικό περιβάλλον, στις βόρειες υπώρειες του όρους Πάρνηθας, διακόπτοντας τη σιδηροδρομική και οδική σύνδεση της πρωτεύουσας με την κεντρική και βόρεια Ελλάδα. Στην εργασία αυτή, ο μηχανισμός της κατολίσθησης προσεγγίζεται αφενός με βάση τα κινηματικά στοιχεία στην επιφάνεια ολίσθησης, τα μορφολογικά επιφανειακά στοιχεία και τα ανυσηματικά στοιχεία της κίνησης και αφετέρου με βάση τη λιθοστρωματογραφία της μάζας που αστόχησε και τα υδρογεωλογικά της χαρακτηριστικά. Με βάση τα ανωτέρω κριτήρια διαχωρίζονται σαφώς στη μάζα της κατολίσθησης τρία διαφορετικά εδαφικά τεμάχια που διαφοροποιούνται ως προς την λιθολογική τους δομή, τα κινηματικά τους χαρακτηριστικά, την παραμόρφωσή τους και την υδρογεωλογική τους συμπεριφορά. Γενεσιουργό αίτιο της εκτεταμένης αστοχίας αποτελεί η διαδοχική απώλεια στήριξης των τριών ανεξάρτητων τεμαχίων

που την συνθέτουν και η ολίσθησή τους επί μίας προδιατεταγμένης επιφάνειας μειωμένων αντοχών, λόγω των εκτεταμένων εκσκαφών στον πόδα της. Τα μόνιμα έργα αποστράγγισης που στόχευαν στην αύξηση του συντελεστή ασφαλείας της κατολισθαίνουσας μάζας και στη σταθεροποίηση της κλιτύς, δεν έλαβαν υπόψη τους την παλαιοτεκτονική δομή, την ανάπτυξη και τη γεωμετρία των γεωλογικών σχηματισμών του στενού και ευρύτερου χώρου της αστοχίας και οδήγησαν σε υπερδιαστασιολόγηση των έργων αποκατάστασης.
Λέξεις κλειδιά: λιθοστρωματογραφία, επώθηση, κινηματική, υπόγεια νερά, σταθεροποίηση κλιτύς.

1. Introduction

The early hours of February the 18th, 1995, an extended landslide occurred in the north roots of Parnitha Mt., at CH. 35+000 of the Athens-Thessaloniki Highway which caused damages to the railway line and the road connection between Athens and northern Greece (Figure 1a). The displaced soil mass swept the Athens-Thessaloniki railway line away, for about 7m downwards, deforming and destroying the gravel ballast in a length of 240m. This movement ended at the deck of the National Highway which leads to Athens, causing serious damages in a length of 80m.

The complex palaeotectonic evolution of the wider area with repeated fold systems, the synclinal and anticlinal structures, and the overthrusts and small-scaled up-thrusts have intensely deformed and altered the schist-sandstone neopalaeozoic formations causing large-scale landslides to the mountainous areas of Parnitha, Kithaironas and Pateras Mountains (Dounas, 1971; Mourtzas et al., 1993).

Cavounidis et al. (1997) describe the general features of the landslide and the proposed remedial measures. Marinou et al. (1997) refer, in general, to the geological features of the landslide and to its hydro-geological regime, while Sotiropoulos et al. (1998) present the results of a 3D groundwater flow study in the vicinity of the rupture surface and examine several draining options at the toe of the slide. Pantelidis and Cavounidis (1997) perform a series of 2D and “pseudo-three dimensional” forward and back slope stability analyses, before and during the occurrence of the failure, as well as after the construction of the proposed remedial measures. Georgopoulos and Vardoulakis (2001) models the sliding mass with a four-rigid body failure mechanism, highlighting the need of draining the soil mass, as the estimated factors of safety, with the consideration of high water table, reveal a slope with limited equilibrium. At the same time the possibility of an extended landslide is examined.

Although it is a geological phenomenon par excellence, in the aforementioned studies it is treated strictly as a geotechnical problem, ignoring important geological features concerning the geology and tectonic environment of the landslide wider area as well as the morphologic and kinematic components which are directly connected with the occurrence and rational remedy of the failure mass.

2. History of the Landslide

2.1. Precursory Phenomena

Enough time before the main landslide occurred, there were clear evidences that the soil mass movements at the level of the Railway line and the Highway had already begun. In May 1993, a small scaled failure occurred at the western end of the Athens-Thessaloniki Highway slope, immediately after its excavation and construction with an inclination of 1:1. In order to confront the failure, slope was reconstructed with an inclination of 1:1.2 and a retaining wall was built at the foot.

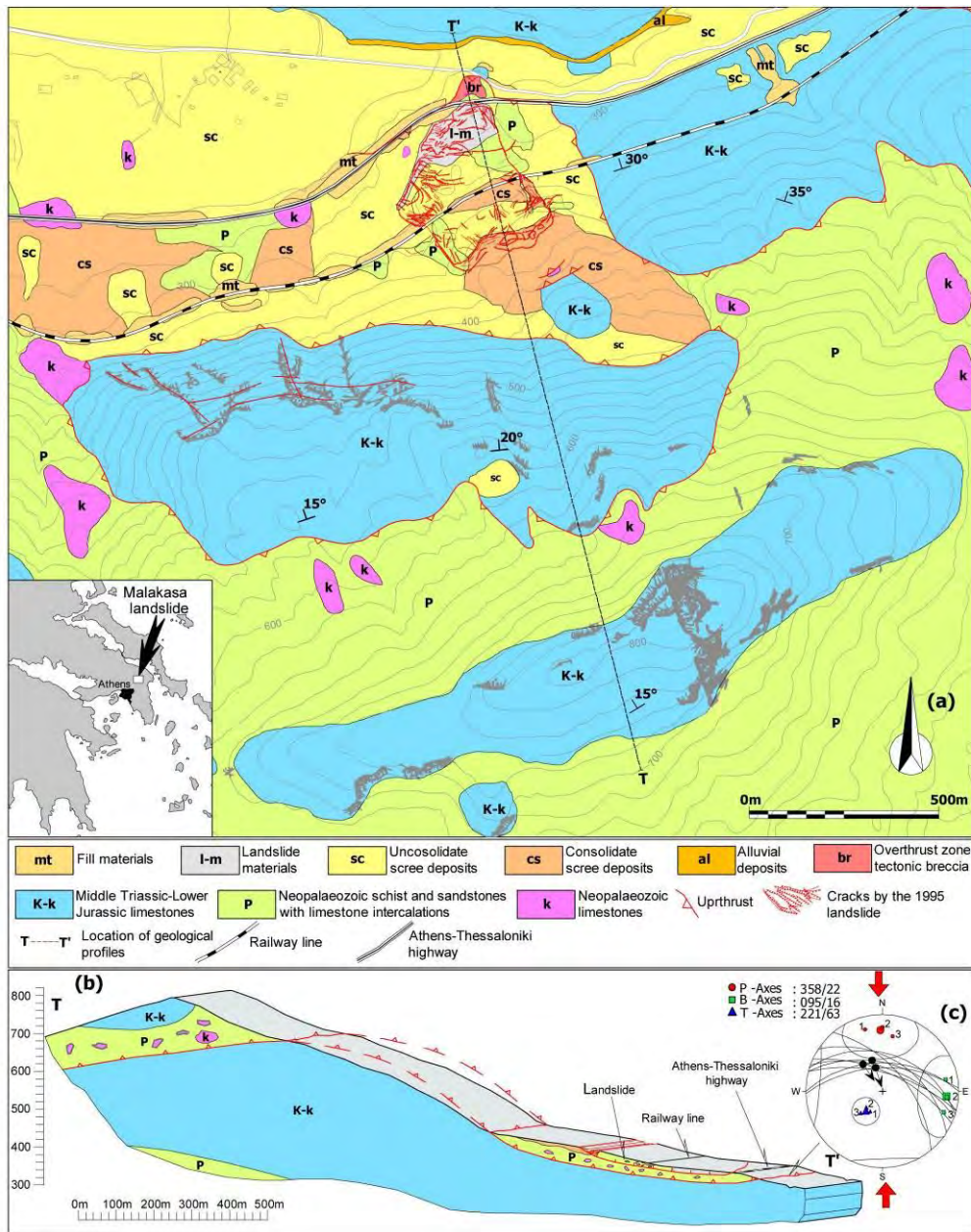


Figure 1 - (a) Location map of Malakasa landslide (b) Detailed geological map of the NE slope of Mt Parnitha in the wider area of Malakasa landslide (c) Geological cross-section along the longitudinal axes of the north-east slope of Mt Parnitha (d) Up-thrust surface data and palaeostress mechanism analysis.

The aforementioned circular failure, being almost 40m wide, which appeared in the western slope of the Highway and the following landslide, which occurred in January 1994, it turned into extended instabilities, with secondary fragmentations downwards of the loose soil mass and spreading of the cracks to the East and upwards, in a 90m long and 20m wide zone, up to the crown of the artificial slope (Figure 2). The landslide caused the detachment of the retaining wall at the joint and its rotation, with maximum vertical and horizontal displacement of 0.1m. It also

caused the failure of two wells. The failure was thought to be small-scaled and it was treated as a local phenomenon. It was assumed that its occurrence was due to the heterogeneity of the lithology, the degradation of the physical and mechanical properties of the materials, and their long-term watering from the spring which was located upwards. Remedial works for the gathering and removal of the spring water took place and the slope angle was reduced to 1:1.5 up to 1:2, with a 4m wide bench in the middle. Also, an embankment, as a foundation for the adjacent road, was constructed and series of piles of 1m in diameter and 12m-14m in length were installed in the slope toe in order to improve the soil (technical report - OMETE S.A., 1994).

From January 1995 up to February 1995, continuous anomalies on the general plan of the railway line, failure of monitoring points which were located in the masonry retaining wall for the protection of the railway, and development and gradual expansion of cracks on the wall were reported. A small local failure occurred after an initial remedial measure which included the excavation of the upwards slope. During the reclamation actions, moisture appeared in a 15m wide zone in the slope and water was gushing from it.

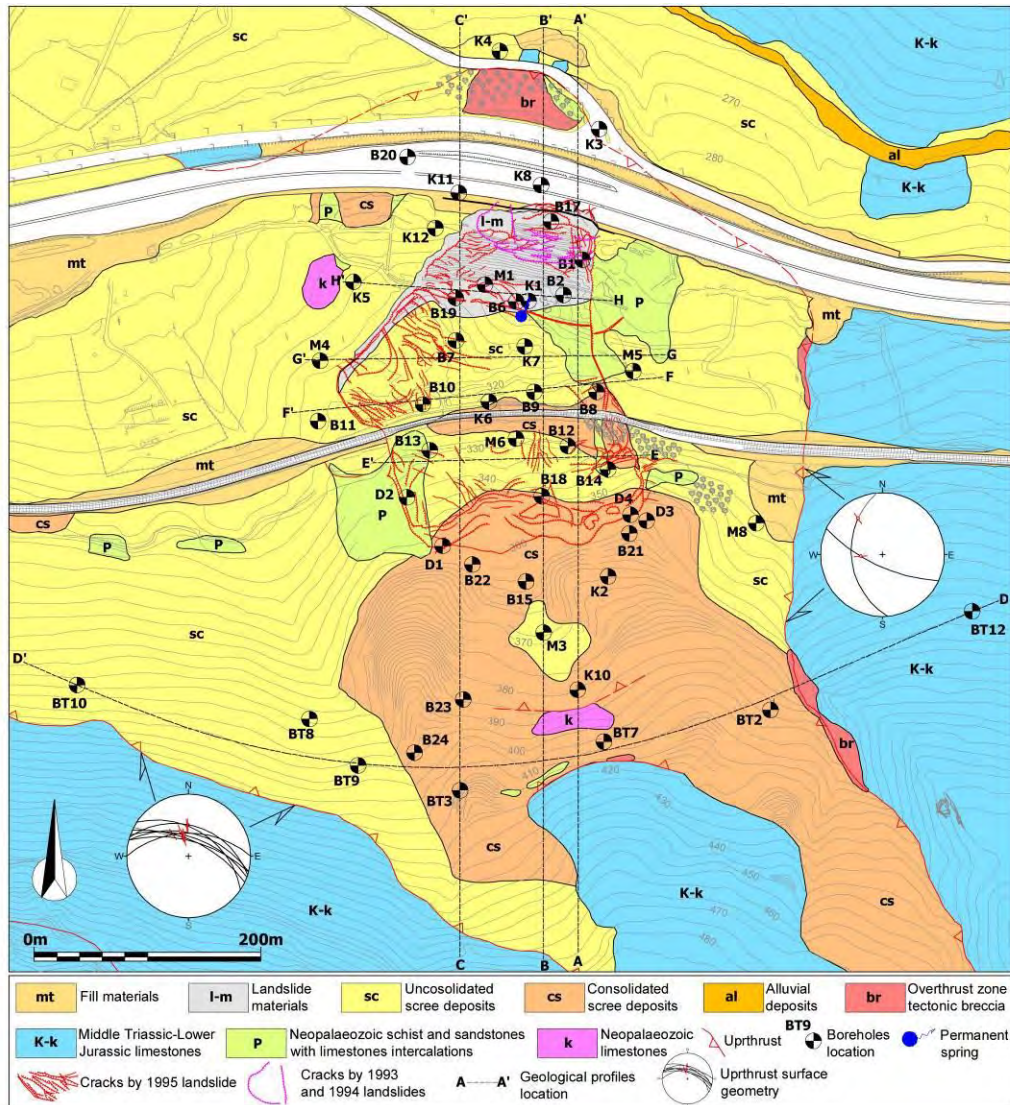


Figure 2 - Detailed geological map of Malakasa landslide.

2.2. Main Landslide Event

In the afternoon of February 16th, 1995, the emergency lane of the highway was lifted by 0.1m, in a 5m wide zone, and within the next few hours the lift was 0.2m and it was spread in all its width. The landslide was activated during the night of February the 18th, 1995. The upwards slope of the highway was cut off by the failure in an altitude of 360m and the 310m long and 240m wide soil mass slid downwards, lifting the main highway lane by 3m up to the position of the New Jersey barrier which was displaced by 3m in plan and finally overturned.

3. Tectonic Structure and Evolution of the Landslide Area

The thrust of the neopalaeozoic formations to the Triassic limestones constitutes the main palaeotectonic structure of the landslide area. This large-scale tectonic movement took place during the first orogenic phase and affected the wider area. It caused strong foliation of the geological formations, with the strike of the main fold axis being NNW-SSE, and the generation of tangential forces that pushed the schist-sandstones towards a SE direction over the carbonate formations of the Sub-Pelagonian geotectonic unit. The following erosion removed significant parts of the tectonically overlying schist-sandstone formations and revealed the younger underlying carbonate bedrock in the form of a “tectonic window”. Also, the erosion caused the fragmentation of the nappes into klippe which lay on the Triassic substratum. The Malakasa landslide occurred in one of these klippe (Figures 1 and 2).

The result of the intense tectonic deformation of the neopalaeozoic sediments is their weathering, alteration, and total loss of their initial structure in some positions, as well as the fragmentation of the inflexible gray sandstone and contained limestone bodies. The slickenside of the thrust has an inclination of 50° – 65° to the NE, while the tectonic glide lines on its surface reveal a compressive movement with orientation of the slide to the SE (Figures 1d and 2). At least another two of the small-scaled thrusts, in the schist-sandstone mass, have similar geometrical features on their slickenside with those of the main thrust. These determine two clearly identified pre-sheared surfaces in the material (Figure 3). The mylonites and fault breccias of the main and secondary thrusts are the result of the mechanical stress on the rocks. The most recent tectonic structure of the area, which has orientation WNW – ESE and forms the steep landscape of the north borders of Mt Parnitha, is the rupture zone “Malakasa – Avlona” and it passes through the south side of the landslide upwards area.

4. Lithostratigraphy of the Landslide Area

The lithostratigraphy of the landslide area was determined based on the results from the geological investigation and geological mapping, made on a scale of 1:5000 and 1:1000, as well as on the data coming from the drillings and testing of the cores (Figures 2 and 3).

The Triassic limestones and the up-thrusted neopalaeozoic formations constitute the Alpine substratum of the wider landslide area, while the oldest and youngest phases of the colluvial deposits, covering the bedrock, constitute the most recent formations. The remainders of the neopalaeozoic nappe, which cover the Triassic limestones in the landslide area, consist of alternation of highly eroded schist-sandstones, shales, and mica schists, which have lost their initial structure and are present in the form of gravels, medium plastic clays, clayey sands, and clayey gravels. They are soft to very soft materials with olive-green, green and gray-green colours. They have been transformed into graphitic schists with intense abrasion and dark or dark-grey colours in deeper layers, and they are presented as clayey sands and sandy clays with medium plasticity, very soft and of medium cohesiveness, as well as silty sands and clayey sands and gravels with sandstone fragments. The former are arkoses of grey to dark colours which are crossed by light-coloured calcite veins (Figures 2 and 3).

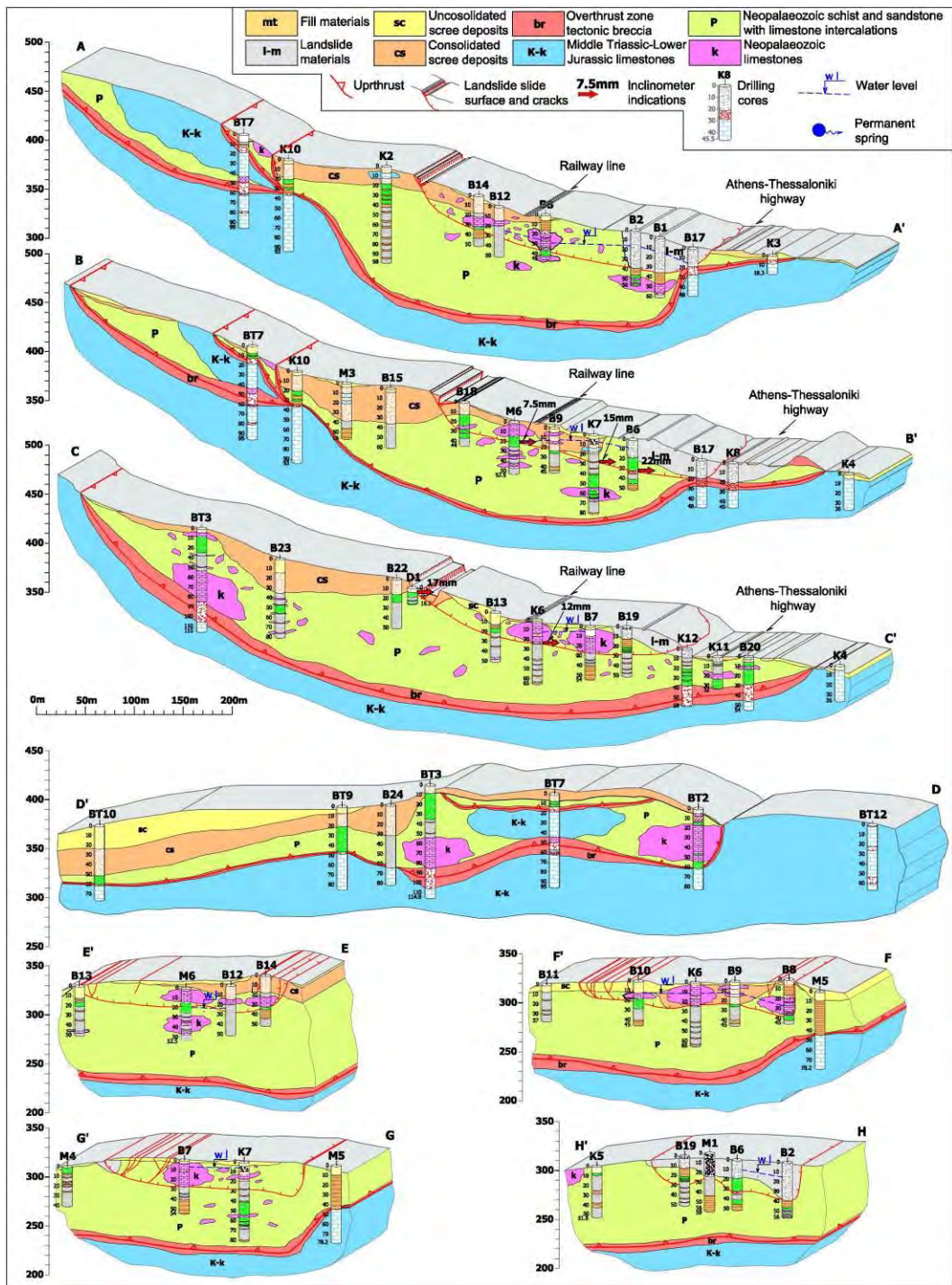


Figure 3 - Geological cross-section of Malakasa landslide.

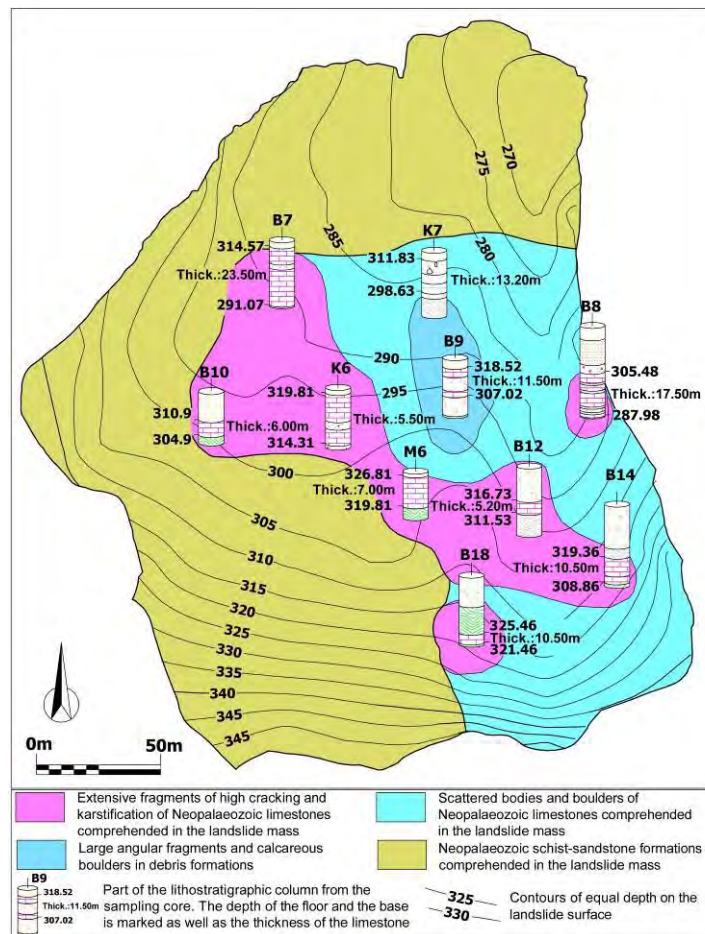


Figure 4 - Dispersion map of the limestone bodies in the mass of the landslide.

The limestone bodies are thinly bedded with intense folding and medium to high fragmentation and karstification. The discontinuities and karstic voids of the rock mass are filled by green clays and clayey sands. The largest proportion of RQD index values is between 0% and 20%. At least three large limestone bodies are contained in the schist-sandstone mass. The first one is about 40m thick and can be found in the western section of the up-thrusted mass, 170m upwards and NE of the landslide head. The second is about 35m thick and it is located 200m upwards and to the north of the landslide head. Finally, the third is located in the central section of the landslide, having NW-SE direction, extends up to a depth of 3m, and has a length of 195m and maximum width of 70m. Its thickness reaches 24m in its NW end, 5 to 7m in the most extended central section, and 10m in its SE end, while its volume is estimated at 216,000 m³. The two smaller limestone bodies, in the north-eastern and southern sides of the main section, are about 25 to 30m long and are having a thickness of 10 and 17m respectively, while their total volume is estimated at 33,000 m³ (Figure 4).

The Upper Triassic limestones are white, grey-white, grey and locally brown in colour. They are unsorted and present high and extremely high strength. At positions they are highly fractured and significantly karstified, in the form of rillenkarren and karstic voids of 4m to 6m in diameter. The filling material contains calcareous fragments and gravels, while it consists of clayey to clayey sandy material and calcareous clay with, locally, high degree of cementation. Two main joint systems cross the calcareous formation in NNE-SSW and NW-SE orientation and dips from 70° to 90°, while the largest proportion of RQD index values is between 20% and 50%. The fault breccia

of the thrust zone consists of calcareous clays, red, pale yellow, off-white, brown-red and dark red in colour, which contain calcareous and shaly fragments and gravels with size 0.02 to 0.15m in varying proportions. It is a highly cemented formation of significant strength which is crossed by sequential surfaces of tectonic slip and its thickness is 20m. It is presented as clayey-silty sand, clayey sand, clayey sand-gravel or clayey-silty gravel of medium plasticity, where it is strongly tectonized and weathered.

The schist-sandstone bedrock is covered by cemented colluvial deposits which consist of calcareous fragments, gravels and angular rock pieces with size 0.02m-0.4m. These are strongly cemented in a matrix which is composed by calcitic-sandstoned, sandy-marly, and clayish-marly material in red to maroon colour and it presents great strength, high degree of fragmentation, and joints with great length and openings with calcareous material on their walls. The erosion along the discontinuities and the gaps from the erosion and from the joints, have induced a great secondary permeability and the fluctuation of the water level, which infiltrates and is stored into the underlying limestones. Finally, the loose colluvial deposits are slope deposits of low strength, consisting of gravels, granular fragments, and boulders of limestones in fine grained material with significant thickness in some places. They are characterized as sandy clays, clayey sands or clayey sands and gravels of medium plasticity.

5. Morphological Features of the Landslide

The mountainous, bold to rugged morphological relief dominates the NNE ending of Parnitha Mt., near the landslide area. As a result of the karstification, vertical dissection, and following erosion, there are steep slopes and vertical stream walls. The relief becomes smooth where the neopalaeozoic schist-sandstones dominate, due to their uniform erosion and the ease of weathering (Figures 1b and 1c). A small “horseshoe” order of the contour lines and a rapid normalization of the relief, in accordance to the mean upwards slope angle of 25°, for a 65m wide zone with sub-horizontal morphology and small inclination of 10° to the North, discerns in the upwards area and in all the width of the landslide head, in altitudes between +360 and +345 meters above principal datum. A small hill is formed at the north side of the landslide toe, downwards the diversion of the NR, by a reflective smooth and concave surface which dips 35° to the S or SSW and has glide lines on it. The inclination of the soil mass, in the intermediate morphology, is 20° to the N at the upwards section of the railway line and 10° at the downwards one. A small morphological crest, which is developed on a NE-SW axis, is formed at the western side of the central section of the landslide, downwards the railway line. The morphology refers to an old landslide, which was developed in the flat between the altitudes of +360 and +345 meters, and its toe ended up to the rising ground, downwards the NR, which stopped its progress and acted as a buttress.

The landslide presents classic tensile cracks at the head, with almost vertical walls and vertical displacement of few meters. These cracks turned into trench gaps, after the mass movement, being 15m to 30m wide and 15m deep. At its sides, the landslide is clearly defined by continual cracks which revealed the failure surface with characteristic glide lines to the direction of the movement. There is, also, intense ground elevation at the landslide toe and multiple failure surfaces, extremely smooth and with glide lines, in different levels (Figure 3).

6. Inclinator Measurements – Determination of the Failure Surface

Fifteen (15) sampling boreholes, supplied with inclinometer tubes, carried out in the area for the observation of the soil mass movements, six (6) of them within failure zone limits and nine (9) out of it. After seven repeated measurements, which took place within nine months, the movement vectors from the inclinometers showed that only some of them presented systematic movement, although within the limits of the instrument error. Movements were located by the inclination tubes in borehole GK1, in the depth of 30.50m (21.50mm), in GK6, in the depth of 22.30m (13.00mm), in GK7, in a depth of 28.20m (15.00mm) and in GM1, in the depth of 26.50m

(11.50mm). Finally, the inclinometer which was installed in borehole D1, in the west end of the landslide head, showed maximum movement of 17mm in the depth of 3.50m, in a time period of 104 days (Figures 3 and 4).

Older sequential failure surfaces, with similar geometric and kinematic features with the recent one, are located on calcareous crusts of core drillings, as well as at the edge and toe of the south slope of the outcrop, downwards the new highway. These surfaces reveal the secondary nature of the landslide because of the pre-existence of a zone of low shear strength with continual activations in the past.

7. Data from the Surface Deformation

The total number of cracks recorded on the sliding mass surface was 114 and the sequential measurements of their position and size did not give clear results for the direction and magnitude of the movement. The variations of their size did not seem to come from factors related to the soil mass movement but they can be attributed to conditions that affect the soil surface. However, the presence, density, and orientation of the cracks on the landslide surface provide significant evidence about the movement of the soil mass (Figures 2 and 5).

By the dispersion of the cracks at the failure surface, the following conclusions are reached:

- The absence of cracks in the central and eastern section of the landslide reveals the solid nature of the block and its movement into one block.
- The large number of cracks, which are located at the west side of the central section and at the toe of the landslide, reveals that they are developed in an area of compression which has, almost, transverse orientation in regard to the landslide boundaries and the direction of movement, as it appears from the glide lines, due to the blocks movement halt.
- The tensile cracks in the area between the head of the landslide and the railway line are parallel or almost parallel to the lateral boundaries of the landslides.

8. Data from the Kinematic Analysis of the Landslide

According to the geometric data of the movement, the tension and compression zones of the landslide, the orientation of the tensile and compressive axes, and the direction of the movement, in every location, are determined (Figure 5). An extended tension zone was determined at the SE side and the central section of the landslide mass, upwards and downwards the railway line. At its north section, failure surface dips to the NW and glide lines have NNE direction and NW-SE orientation of the tension axis (Tension area II). At the NE side of the landslide, movement took place on a surface dipping to the ESE, glide lines with NNE and NE direction, determining a zone of compressive events with orientation of the compressive axis to the NE-SW (Compressive area II). At least two older slip planes, with striations that have the same orientation as the recent ones, were determined at the sequential planes of the calc-crust, at the SE end of the compressive area II. At the SW section of the landslide, upwards the railway line, a tension zone was determined with tension axis orientation N-S and mass movement to the NNW at the most southern part, to the North at the middle part, and to the NNE when approaching the railway line (Tension area III). A compression zone by sequential compressive cracks was determined immediately downwards the morphological crest, which has planes with SW inclination and glide lines to the ENE (Compressive area III).

A limited extended tension area is formed at the NW end of the landslide toe, exactly where tension cracks occurred by the 1993 and 1994 failures. Slip planes, in this area, incline to NNE, N and NNW, while one inclines to the NW, by dispensation, with glide lines oriented to the N and direction of the tension axis to the NNW-SSE (Tension area I).

The NW end of the landslide toe is been dominated by compressive events, with sequential planes that incline to the SW, glide lines with NE direction and compressive axis with NE-SW orientation (Compressive area I).

The calcareous surface at the north slope of the morphological outcrop downwards the National Road inclines to the SSW with glide lines which are headed to the NNE and compressive axis of NNE-SSW orientation. So, it is confirmed that the geometrical features of older soil mass activations in the area of the landslide toe are barely different from the recent one.

In conclusion, tension area (I) with compressive area (I), tension area (II) with compressive area (II), and tension area (II) with compressive area (III) define three different soil blocks of the unstable mass (Figure 5).

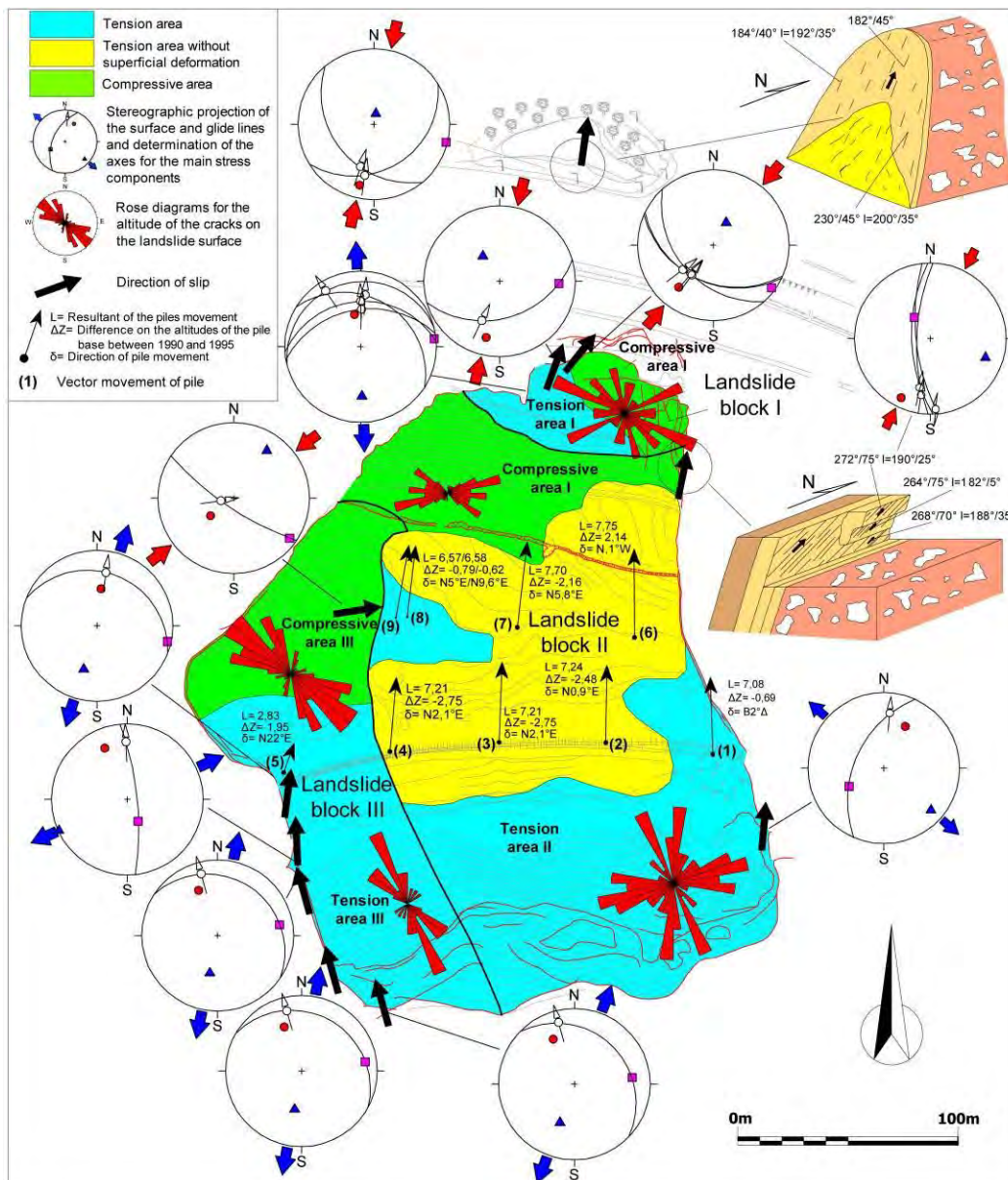


Figure 5 - Kinematic analysis of the landslide.

9. Kinematics of the Landslide

Based on the aerial photographs taken before (9/21/1987) and after (2/21/1995) the occurrence of the landslide, the photogrammetric impression of the greatest landslide area was drawn up, with the determination of 12 ground control points through satellite Global Positioning System (GPS) (Figure 5).

The comparison of the two maps gives significant information about the morphology of the area before the widening of the National Road and after the occurrence of the landslide. The dense forest cover at some parts of the area does not allow the determination of the exact movement vectors with desirable accuracy. However, due to the existence of ten telegraph poles along and in a distance 50m downwards the railway line, the accurate measurement of the vectorial movement was possible.

Two areas with distinct kinematic can be clearly defined by the movement vectors. The area which includes the western section of the landslide is defined by the poles 14 (5) and 5 (8) and the western boundary of the sliding mass (Figure 5). This section has been moved by 2.83m to the NE. The eastern section of the landslide shows its maximum movement at the central part, from 7.21m up to 7.75m, reducing at 6.57m up to 7.08m in its western and eastern margin. On the other hand, the eastern section of the landslide is divided, considering the direction of movement, into the western part, to the west of the poles 12 (3) and 6 (7) with a movement direction to the NNE, and the eastern part with a movement direction to the NNW (Figure 5).

10. Hydro-geological Conditions of the Landslide Mass

The spread of the Triassic and Neopalaeozoic limestone phases of the Parnitha Mt. favors the development of a rich karstic underground water potential. The spring at the landslide mass, in the altitude of +313 and with constant flow of $1.5\text{m}^3/\text{h}$ to $2\text{m}^3/\text{h}$, is an overflow spring and gushes out at the contact between the entrapped, highly cracked, karstic, Palaeozoic, calcareous blocks and the impermeable schist-sandstone bedrock. Also, the discharge of high quantities of water during the winter, at the wider spring area and the slope upwards the railway line, shows the existence of a significant, unsteady, hydraulic load in the landslide mass, whose volume depends on the rainfall (Figure 2). The underground karstic aquifer is developed in the central section of the landslide, between the elevation contour lines of +335, at the railway line area, and +310, at the drainage cemented trench. From the piezometer measurements in 42 vertical drillings, distributed in three parallel to the motorway axis branches and a conjunctive vertical branch, arises that the groundwater table varies between 2.00 and 35.11 meters from the surface (Figure 6a). In the central and most extended section of the aquiferous zone, the piezometric level ranges between +305 and +310 and reduces sharp to the NW in +282 and smoothly to the South in +304, displaying a small mean hydraulic gradient of 5° to the North (Figure 6b).

The groundwater in the central section of the landslide mass forms a significant hydraulic head above the failure surface with a volume of 500.000m^3 . The distribution of the hydraulic head is not uniform, so there are four distinct areas which are recognized. At the northern section of the aquiferous zone, the hydraulic head is over 20m, at the central section is between 10m and 20m, at the southern and the eastern sections is between 0m and 10m, while at the southern and eastern margins the piezometric surface is lower than the failure surface (Figure 6c).

The pumping tests, which carried out at the vertical drillings for the degradation of the piezometric level, revealed high drainage volumes and recharge rates at the section with the highest piezometric level and hydraulic head (KG5 to KG9), in relation to the rest of the drillings which had low drainage volumes and slower recharge. The drainage at the west side drillings, downwards the railway line (EY11 and EY12), was achieved by 50% of the desirable, at those of the east side (B2, EY1 and EY8) by 40%, while at the central section drainage did not exceed 15%. Also, the

discontinuity of the impermeable beddings does not allow the hydraulic contact even between neighbouring drillings.

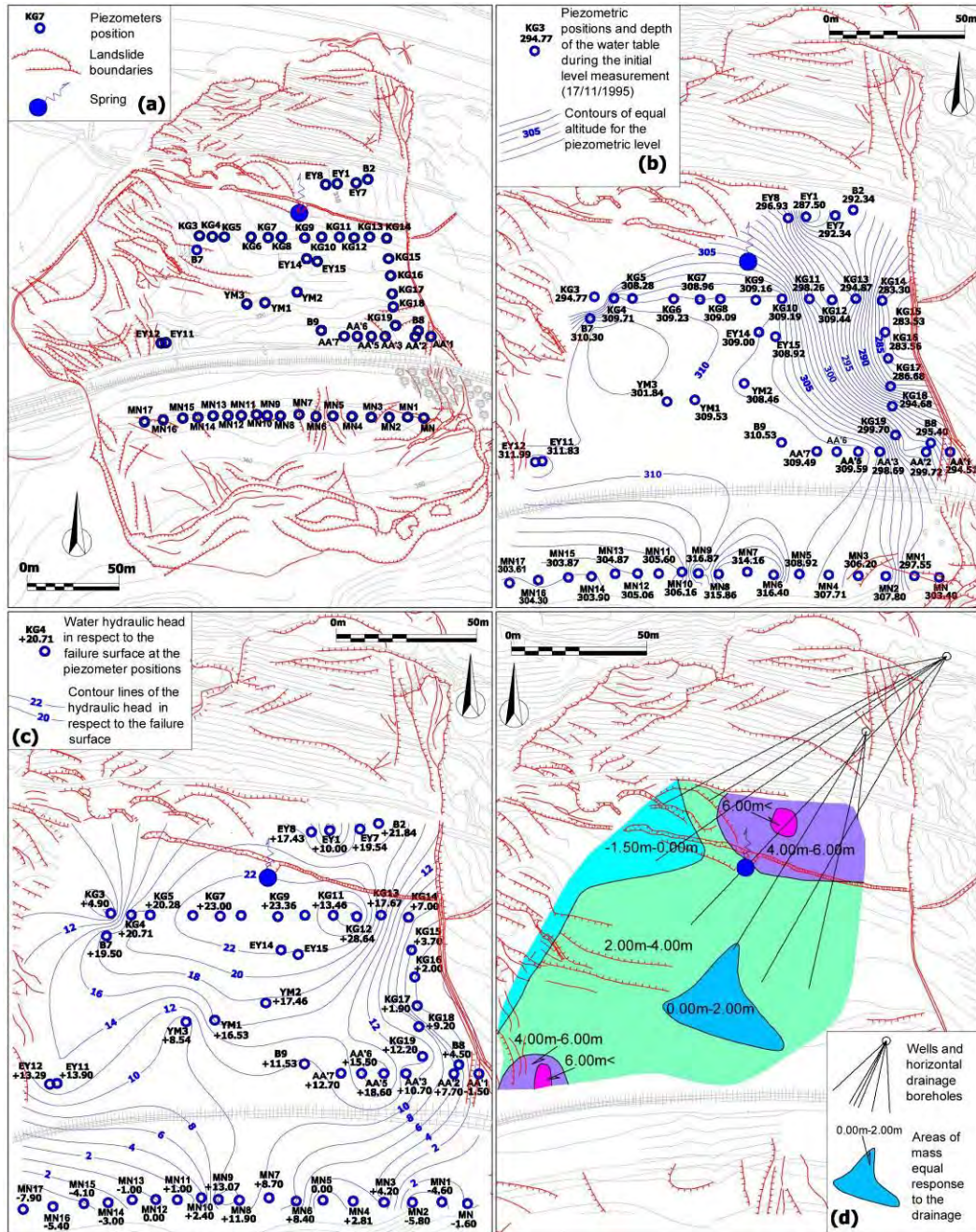


Figure 6 - Maps of groundwater conditions in the Malakasa landslide. (a) Distribution of Casagrande type piezometers in the landslide mass. (b) Piezometric map of Malakasa landslide. (c) Potentially groundwater pressures on the slide rupture surface. (d) Response in the draining at the different locations in the slide mass by placing horizontal drains

Twelve horizontal drillings were executed in two positions through equal number of shafts, 3 and 8 meters deep, and they extended from 10 to 150 meters. Discharge, in both shafts, varied between 1 and 8m³/h.

The response to the drainage was different from place to place. The western side of the central section of the landslide showed degradation of the piezometric level between 0m and 9m, while at the rest of the western side the piezometric level increased up to 1.5m. Consequently, there is a clear discrimination into two areas, one of increased ground water capacity, high hydraulic head, increased discharge volumes and quick recharge, at the central section of the aquifer zone, and one area of decreased respective hydraulic parameters at the eastern and northern borders (Figure 6d).

11. Data Evaluation

The landslide mechanism been approached, on the one hand based on the kinematic features, morphological superficial data and vectorial features of the movement, and on the other hand on the lithostratigraphy of the failure mass and its hydro-geological features. Based on these criteria, there is clear discrimination of the landslide mass into two different blocks, which are differentiated by their lithological structure, kinematic features, deformation and hydro-geological behaviour (Figure 7). The sudden detachment and downwards movement of the extended soil mass of 1,300,000m³ volume, in the 18th of February 1995, at the Kilometer Post (KP) 35+000 of the new National Highway Athens – Thessaloniki, occurred in an area of intensive palaeotectonic processes. The Neopalaeozoic schist-sandstone formations with extended limestone bodies in their mass and in the greater landslide area are up-thrusted to the Triassic limestones, are highly cracked, eroded, and have been turned into clay with total loss of their initial structure at positions.

The main front of the thrust has surfaces which incline to the NE, with angles between 60° and 65° and lines which refer to a compressive movement with direction of sliding to the SE. This front, actually, defines the schist-sandstone klippe in which the failure occurred from the North. At its western boundaries, it is developed in NW-SE up to NNW-SSE direction, with surfaces which incline to the SW up to WSW and with angles between 50° and 75°, respectively. Another two up-thrusted events, in the schist-sandstone mass, present similar geometrical features with the main fronts of the thrust and have caused extra fatigue to the neopalaeozoic formations.

The landslide mass was separated into two distinct blocks: (i) to the eastern, and most extended block, with estimated volume of 993,000m³, where the significantly folded and fractured, permeable calcareous mass of estimated volume 250,000m³ develops on the tectonically stressed and impermeable schist-sandstone mass and (ii) to the longitudinal western block of limited extend, with estimated volume 225,000m³, where there are, exclusively, soil layers with increased permeability (Figure 7). The eastern block moved totally and independently, in respect to the western one, at NNE up to NE direction, with total horizontal movement of 7m and vertical movement of 2.50m. The tension and compressive cracks at the head and toe of the slope, respectively, accumulated at the periphery of the sliding mass and were totally absent from the central section due to its rigid nature. The western part of the sliding mass made up a distinct soil mass with independent spatial and temporal resultant movement to the North, total horizontal movement of 3m and vertical movement of 2m. The differential movement of 4m between the two fragments was covered through the numerous and dispersed cracks of the western section. The southern part of the eastern block seems to be an independent block which has boundaries that coincides with the failure of 1994. This soil block, with estimated volume of 63,000m³, moved in NW up to NNW direction with clockwise sliding component, pushed by the upward section of the landslide (Figure 7).

From the discharge of the horizontal drainage drillings, which perforate the sliding mass radically in order to unload it, the great potential of the calcareous aquifer was determined, with the discharge flows being over 100 times than the one of the western section (Figure 7). The sequential older failure surfaces, which were determined to the NE end of the landslide and in

drilling cores, as well as to the calcite surface, which covers the southern slopes of the morphological outcrop, downwards the NR, with geometric and kinematic features in respect to these of the recent one, show the presence of a zone with low shear strength (residual strength) and the secondary nature of the sliding.

The gradual loss of support, caused by the sequential excavations in the slope toe made in a length of 110m, 155m in width and varied depth between 5m and 16m, in combination with the increased hydraulic head of the upward mass, was one of the most important factors for the landslide occurrence (Figure 8).

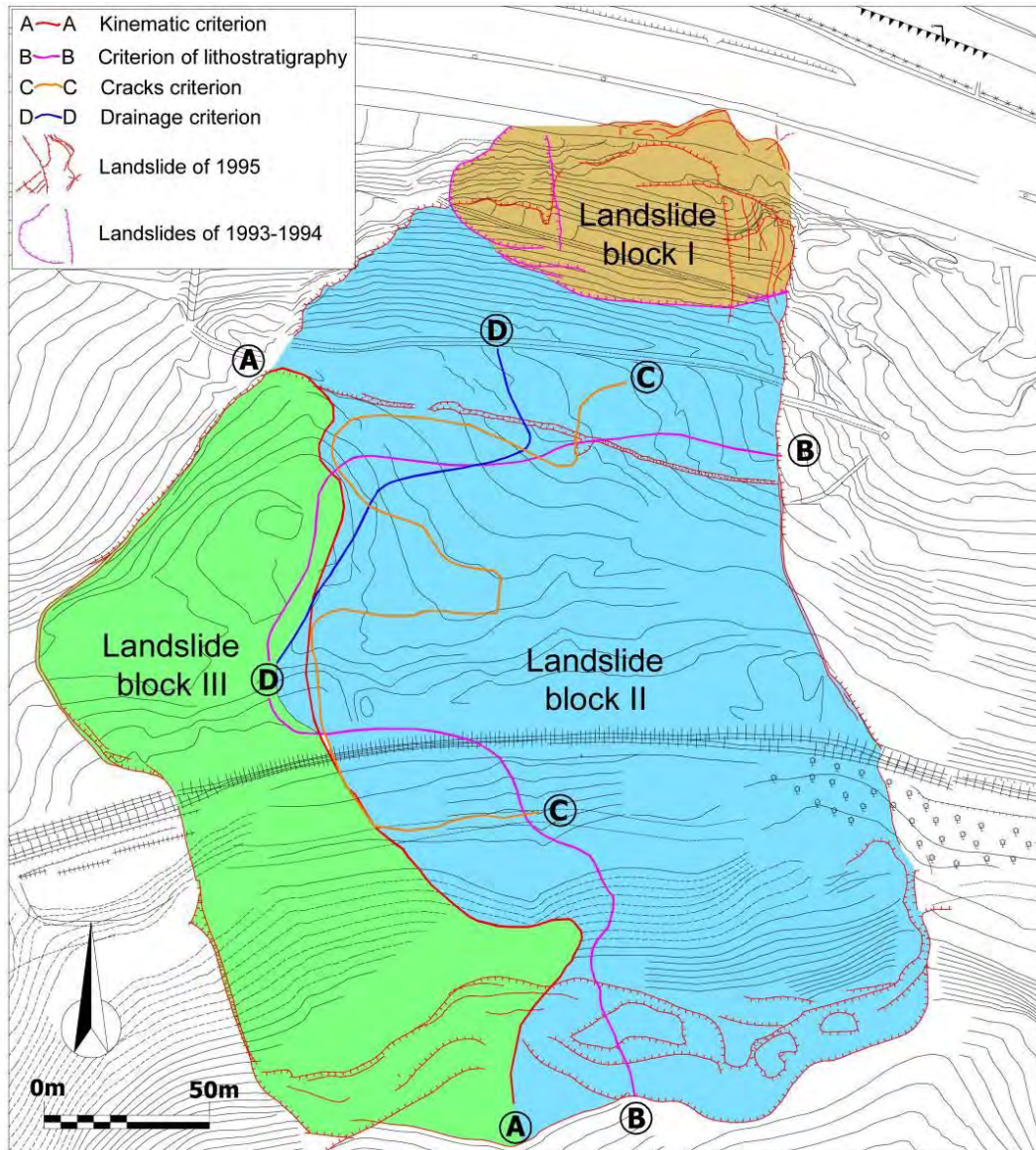


Figure 7 - Delineation criteria of the soil blocks which form the landslide mass.

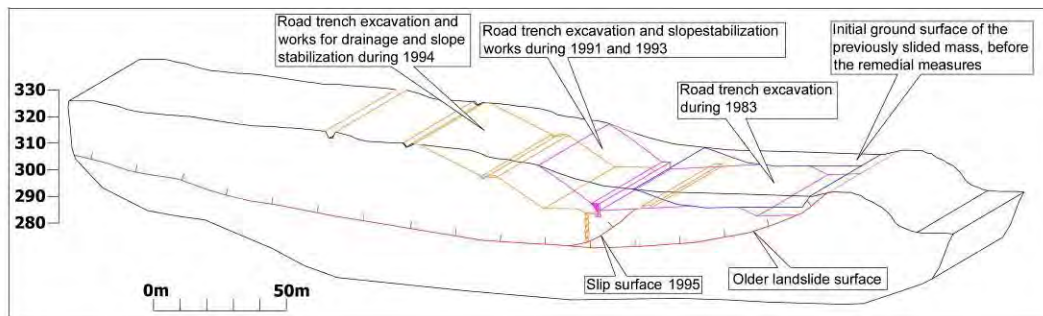


Figure 8 - Representation of the different excavation stages for the figuration of the National Highway at the landslide toe.

12. Conclusions

The evaluation of all data mentioned above lead to a different outlook for the failure mechanism of the landslide. The main causal factor was the gradual loss of support of three independent blocks which form the sliding mass and their slip upon a pre-sheared surface of limited strength.

The extended works for the drainage of the sliding mass included, among others, the construction of an expensive drainage system of tunnels, with one longitudinal and six transverse branches of 1,400m in length. During these works, the Palaeotectonic structure and the development and geometry of the geological formations of the narrow and wider area were not taken into account. The construction of a vertical drainage drilling network in the area of the aquifer zone to a maximum depth of 150m, ending at the Triassic limestones of increased secondary permeability, would ensure the full drainage of the Neopalaeozoic limestone bodies being at the central section of the landslide, with significantly low cost.

13. References

- Cavounidis S., Sotiropoulos E., Vettas P., Avgeropoulos P. and Marinos P. 1997. The Malakasa Landslide. A general review, *Proc. of the 3rd Greek Congress of Geotechnical Engineering*, Patras, Greece, 227-236.
- Dounas A.G. 1971. Geology of the area between Megara and Erithraia village (Attica), *PhD Thesis*, University of Athens, 141pp.
- Georgopoulos I.O. and Vardoulakis I. 2001. Study of the Malakasa Landslide of 18-2-1995 by using Combined Block Failure Mechanisms, *Proc. of the 4th National Congress of Geotechnical Engineering*, Athens, Greece, 403-410.
- Marinos P., Yannatos M., Sotiropoulos E. and Cavounidis S., 1997. Increasing the stability of a failed slope by pumping, Malakasa Landslide, Athens, Greece, in Marinos et al. (eds), *Engineering Geology and the Environment*, Balkema, Rotterdam, 853-857.
- Mourtzas N.D, Kolaiti E. and Papanikolaou P. 1993. Geological Features of the Landslide at Aspropyrgos Area (Attica, Greece), in Anagnostopoulos et al. (eds), *Geotechnical Engineering of Hard Soils-Soft Rocks*, Balkema, Rotterdam, 1137-1146.
- Pantelidis P. and Cavounidis S. 1997. Slope Stability Analyses for Malakasa Landslide. *Proc. of the 3rd Greek Congress of Geotechnical Engineering*, Patras, Greece, 261-268.
- Sotiropoulos E., Dendrou B. and Papanikolaou P. 1998. Groundwater Conditions and Drainage of a Large Slide. *Proc. of the 4th Int. Conf. on Case Histories in Geotechnical Engineering*, 8-15/3/1998, St Louis Missouri, USA, paper No 2.44.